Electronic Supplementary Information

Metallopeptide Nanoreservoirs for Concurrent Imaging and Detoxification of Lead (Pb) from human Retinal Pigment Epithelial (hRPE1) Cells

Aanand Kautu[a, +], Shruti Sharma[a, +], Ramesh Singh[b, #], Saurabh Singh Negi[c], Narendra Singh[d], Narayan Swain[a], Vikas Kumar[e], Nikunj Kumar[c], Puneet Gupta *, [c], Dheeraj Bhatia*, [b] and Khashti B. Joshi*, [a]

[a]. A. Kautu, S. Sharma, N. Swain and Dr. K. B. Joshi*; Department of Chemistry, School of Chemical Science and Technology, Dr. Harisingh Gour Vishwavidyalaya (A Central University), Sagar, MP, 470003, India; E-mail: kbjoshi77@gmail.com; kbjoshi@dhsgsu.ac.in

[b]. Dr. R. Singh, Dr. D. Bhatia, Department of Biological Sciences and Engineering, Indian Institute of Technology, Palaj, Gujarat 382355. E-mail: dhiraj.bhatia@iitgn.ac.in

[c]. S. S. Negi, N. Kumar, Dr. P. Gupta*; Computational Catalysis Centre, Department of Chemistry, Indian Institute of Technology Roorkee, 247667 Uttarakhand, India. E-mail: puneet.gupta@cy.iitr.ac.in

[d]. Dr. N. Singh, Indian Institute of Technology Kanpur, U.P., 208016, India.

[e]. Dr. V. Kumar, Department of Chemistry, Government PG College Khimlasha, M.P.

+ These authors contributed equally to this work.

Current address: Department of Mechanical Engineering, Colorado State University, Fort Collins, CO, US

1.0 Materials and Methods (General): - The solvents and reagents employed in this investigation were obtained from diverse commercial suppliers as per specific requirements. L-Phenylalanine and L-Tyrosine amino acids were procured from Spectrochem in Mumbai, India. 2,6-Pyridinedicarboxylic acid, employed as a linker, was sourced from SRL Pvt. Ltd. in India. Peptide coupling agents, including N, N´-dicyclohexylcarbodiimide (DCC), N-hydroxybenzotriazole (HOBt), and 1-ethyl-3-(3-dimethylaminopropyl) carbodiimide (EDC. HCl), were obtained from Avra Synthesis Pvt. Ltd. in Hyderabad, India. The protecting reagent, Di-tert-butyl dicarbonate (Boc anhydride), and the deprotecting reagent, Trifluoroacetic acid (TFA), were sourced from Spectrochem Pvt. Ltd. Organic bases, such as triethylamine (Et_3N), diisopropylethylamine (DIPEA), and 4-Dimethylamino pyridine (DMAP), were supplied by S D Fine-Chem Ltd. Strong anion exchange resin (Dowex 1-X8) was acquired from HiMedia Laboratories Pvt. Ltd. in India, and strong cation exchange resin (Amberlite IR-120 Na form) was purchased from Spectrochem Pvt. Ltd. in Mumbai, India. Silica gel with mesh sizes of 60-120 and 100-200, along with precoated aluminum sheets for thin-layer chromatography (TLC Silica gel 60 F254), were procured from Merck Chemicals in India. Solvents, including methanol (MeOH), ethanol (EtOH), dichloromethane (DCM), ethyl acetate (EtOAc), acetone (Ac_2O), chloroform ($CHCl_3$), dimethylsulfoxide (DMSO), diethyl ether (Et_2O), acetonitrile (ACN), pyridine, N, N-dimethylformamide (DMF), and tetrahydrofuran (THF), were purchased from S D Fine Chemicals Ltd. in India. Furthermore, HPLC-grade solvents and deuterated solvents for nuclear magnetic resonance (NMR) spectra were sourced from Merck Pvt. Ltd. Metal salts, specifically those of mercury, zinc, cadmium, and lead, were obtained from Himedia Laboratories Pvt. Ltd. in Mumbai, India. All other requisite reagents were secured from HiMedia.

2.0 Peptide Synthesis- The synthesis of tripeptide(Tyr-Phe-Phe) and the C_2-Symmetric pyridine-bis- Tyr-Phe-Phe metallopeptide conjugate MPC was performed by conventional solution phase synthesis via established lab protocol mentioned in

research paper published our group. The purity and identity of these compounds were confirmed before their utilization. All experiments were conducted under ambient room temperature conditions.

3.0 Fluorescence spectroscopy- Fluorescence intensity was assessed at room temperature using an excitation wavelength (λ_{ex}) of 260 nm. The interaction between Tyr-Phe-Phe and MPC-1 with relevant metal ions was individually investigated to discern alterations in their behaviour. Emission spectra were captured within the range of 280 nm to 500 nm. A stock solution of each metal ion salt at a concentration of 15 mM in water was prepared. For each metal ion, the ethanolic solution was titrated with the peptide (20 µM) up to a maximum concentration of 80 µM. Fluorescence spectra were recorded using a Varian Luminescence Cary Eclipse spectrophotometer equipped with a 10 nm quartz cell, while maintaining a controlled temperature of 25 ± 0.1°C. High-performance liquid chromatography (HPLC)-grade water and ethanol were employed in these research endeavours.

4.0 UV studies- UV-Vis absorption spectra were collected using a Lab India UV-VIS Spectrophotometer 3000+ equipped with a 10 mm quartz cell, and the measurements were maintained at a constant temperature of 25±0.1 °C. To initiate the experiment, a stock solution with a concentration of 1 mM for each type of metal ion was meticulously prepared in water. Subsequently, solutions containing 10 µM of both tripeptide and pyridine-bis- Tyr-Phe-Phe Metallopeptide Conjugate (MPC) in ethanol were titrated with each specific metal ion until reaching a final concentration of 200 µM, utilizing the previously mentioned stock solution.

5.0 FT-IR Study- To assess the functional group composition of both the peptides, with and without the presence of metal ions, Fourier-transform infrared (FT-IR) spectra were acquired utilizing a Bruker Alfa II attenuated total reflection (ATR) instrument. The spectral data encompassed the range of 4000-500 cm^{-1}, with a spectral resolution of 4

cm^{-1}, employing 2 sample gain and 32 sample/background scans. Data processing was carried out using OPUS 7.0 software, incorporating noise removal procedures.
A 200 μM solution of MPC, both in the absence and in the presence of metal ions at a 1:3 ratio, was applied and dried onto a ZnSe substrate. Subsequently, the spectral region corresponding to Amide I, ranging from 1700 to 1600 cm^{-1}, underwent deconvolution analysis using Origin software. This deconvolution process was guided by the count of initial peak values derived from the second derivative spectrum. A quantitative evaluation of the area linked to each spectral component was carried out to determine its influence on the secondary structural features.

6.0 Circular Dichroism spectroscopy:- CD spectra were collected between 195 nm to 270 nm and each spectrum was the average of 3-5 scans. All experiments were carried out at 25±0.1 °C. Spectra were recorded at the final concentration of MPC-1 alone and MPC-1+Pb^{2+} at 200 μM, on JASCO J-815 CD SPECTROMETER by using a quartz cuvette with a path length of 1mm. To avoid any instrumental baseline drift between any measurements, the background value was subtracted for each sample measurement with ethanol and ethanol water wherever needed.

7.0 Atomic Force Microscopy (AFM)- The test sample(s) at appropriate concentration were meticulously prepared in a controlled, dust-free environment and deposited onto a freshly cleaved muscovite mica surface. Subsequently, they were subjected to drying under a 60W light bulb for 30 minutes, followed by vacuum drying followed by imaging using an atomic force microscope (AFM) of the INNOVA model, an ICON analytical equipment by Bruker. The AFM operated in both contact and tapping modes, utilizing a cantilever (NSC 12(c) from MikroMasch) featuring a Silicon Nitride Tip managed by NanoDrive™ version 8 software. The cantilever had a resonant frequency of approximately 260 kHz. Imaging was conducted under ambient conditions at a temperature of 25±0.1 °C, with a scan speed ranging from 2 to 1.5 lines per second. Subsequent data analysis was performed employing the Nanoscope Analysis software.

8.0 Scanning Electron Microscopy (SEM)- Scanning Electron Microscopy (SEM) images were acquired using a FEI QUANTA 200 microscope equipped with a tungsten filament gun. The microscope was set to a working distance of 4.0 mm and operated at a voltage of 7.99 kV. A minute volume (10 μL) of, MPC-1 at 200 μM concentrations was delicately deposited onto the designated surface(s) and allowed to undergo overnight air drying at room temperature. Subsequently, it underwent an additional phase of drying under high vacuum conditions lasting 30 minutes. The specimen was then subjected to a 1-minute gold coating process and subsequently observed using SEM.

9.0 Transmission Electron Microscopy (TEM):- In accordance with established protocols for Transmission Electron Microscopy (TEM) sample preparation, a freshly prepared 10 μL solution of 200 μM concetration was meticulously dispensed onto a copper grid that had been coated with a carbon layer featuring a mesh size of 200. Any surplus sample was delicately eliminated from the grid, and the residual specimen was permitted to undergo an air-drying process at room temperature for duration of 6 hours. The samples were subsequently subjected to examination utilizing a FEI Titan G2 60-300 Transmission Electron Microscope (TEM).

10.0 Confocal microscopy- Cellular specimens affixed to glass substrates were subjected to comprehensive examination through the utilization of a Leica TCS SP8 confocal scanning laser microscope. The selective excitation of distinct fluorophores was achieved through laser emissions of specific wavelengths: 405 nm for 4',6-diamidino-2-phenylindole (DAPI) and 488 nm for phalloidin. Subsequently, image analysis was meticulously conducted employing the Fiji ImageJ software, facilitating the precise removal of background signal artifacts and the subsequent quantification of cellular intensity and area measurements. A systematic quantification protocol was applied to 30 to 40 individual cells. The resulting dataset, comprising only validated and rigorously assessed data points, was then subjected to graphic representation using the

GraphPad Prism software, aligning with the established practices of highly reputable journals within the biological sciences.

11.0 Cell Culture and Treatment:- For the cellular uptake experiment, the RPE1 cells were cultured in DMEM containing 10% fetal bovine serum and antibiotic at 37 °C with 5% CO_2 in a humidified incubator. Approximately $1x10^5$ cell counts per well were seeded on a glass coverslip in a 6-well plate overnight. Before treatment, the seeded cells were washed with 1× PBS buffer three times. After washing, the cells were treated with Pb^{2+} salt solution (500nm) and Pb^{2+} ions +peptide (1:1) for 24h. The treated cells were fixed for 15 min at 37 °C with 4% paraformaldehyde and rinsed three times with 1×-PBS. The cells were then permeabilized with 0.1% Triton-X100 and stained with 0.1% Alexa Fluor™ 488 phalloidin to visualize the actin filaments. Then the cells were washed three times with 1× PBS and mounted onto the slides with Mowiol and DAPI to stain the nucleus.

12.0 Computational studies/ Details: Calculations were executed utilizing the ORCA quantum chemical program package. Geometries were optimized using the GGA density functional BP86 and def2-SVP basis sets. Non-covalent interactions were considered through dispersion corrections (D3) with Becke-Johnson (BJ) damping. Subsequent numerical frequency calculations were performed on optimized geometries to ensure they represent stationary points with no imaginary frequencies. Binding energies were determined through single-point calculations using the BP86/def2-TZVP/C-PCM(EtOH) method applied to BP86/def2-SVP geometries(references cited).

13.0 MTT Assay: An MTT assay was performed to evaluate the cytotoxicity of the synthesized peptide, lead(II) ions (Pb(II)), and the peptide-Pb(II) conjugate on human retinal pigment epithelial (RPE-1) cells. RPE-1 cells were seeded in a 96-well plate at a density of 20,000 cells per well and incubated for 24 hours at 37°C to allow for cell attachment and recovery. Subsequently, the cells in different wells were treated with

the peptide, Pb(II), and the peptide-Pb(II) conjugate at a concentration of 500 nM, while untreated cells served as a control group. Following an additional 24-hour incubation at 37°C, a solution of 3-(4,5-dimethylthiazol-2-yl)-2,5-diphenyltetrazolium bromide (MTT) was added to each well, and the plates were incubated for 4 hours to allow viable cells to metabolize the MTT and form insoluble formazan crystals. The MTT solution was then removed, and dimethyl sulfoxide (DMSO) was added to solubilize the formazan crystals. After a 15-minute incubation in the dark, the absorbance of the resulting coloured solution was measured at 570 nm using a multi-well microplate reader, with higher absorbance values indicating greater cell viability.

14.0 Figures:

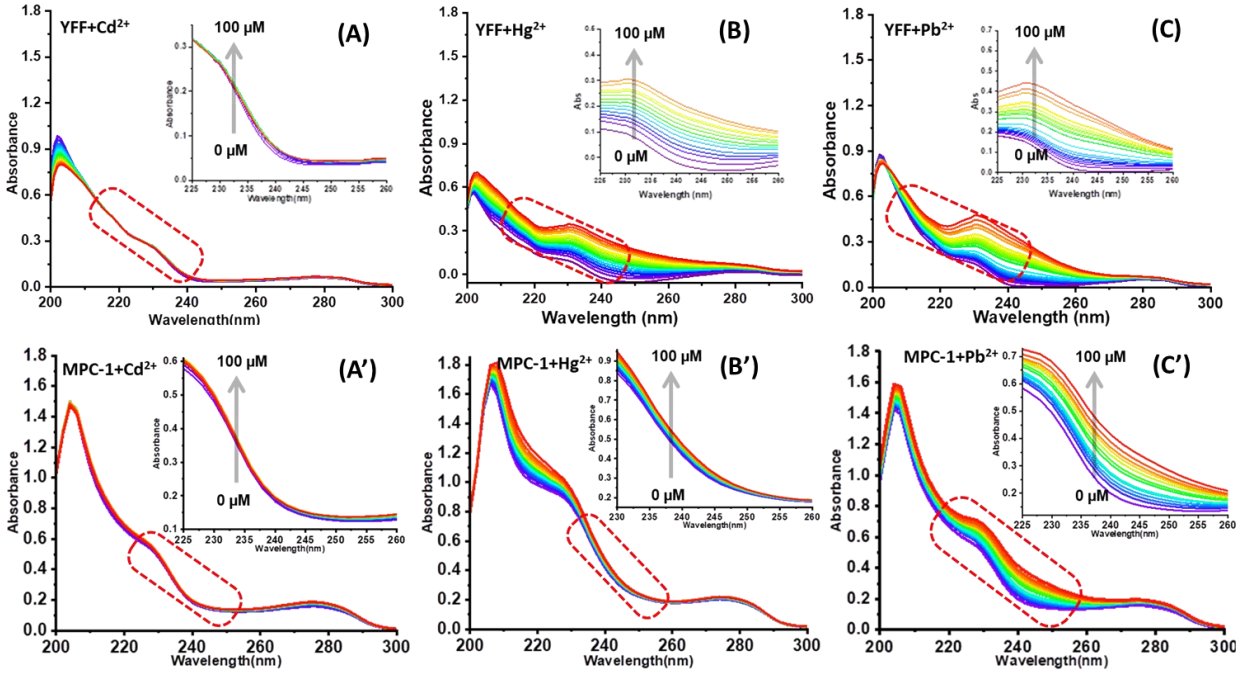

Figure S1: UV-Vis titration spectra illustrating the impact of the gradual addition of Cd^{2+} ions (A, A′), Hg^{2+} ions (B, B′), and Pb^{2+} ions (C, C′) (1 mM) on tripeptide and MPC respectively. The spectra show the increase in absorbance intensity of the aromatic sidechain, acid and amide region.

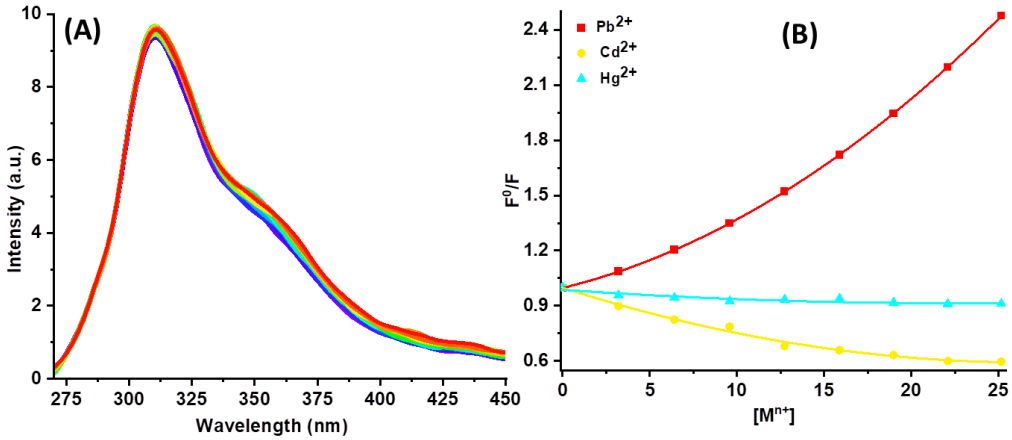

Figure S2: (A) Fluorescence emission spectra of MPC-1 with the gradual addition of Hg^{2+} ions (λ_{ex} = 260 nm). (B) Stern-Volmer plots illustrate the competitive complexation of MPC-1 with Pb^{2+}, Cd^{2+}, and Hg^{2+} ions.

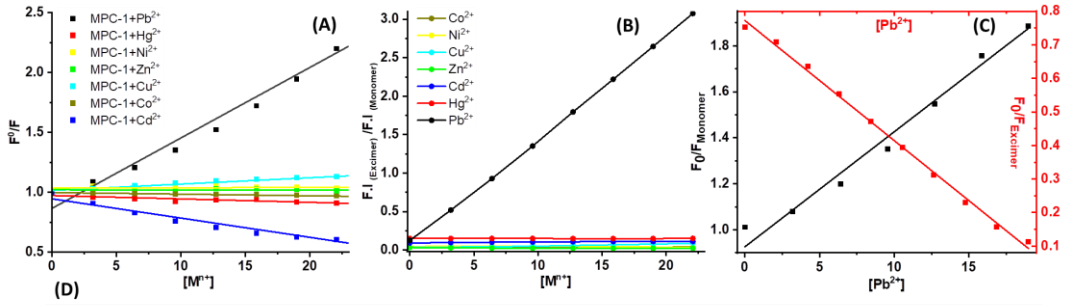

Metals	Pb^{2+}	Hg^{2+}	Cd^{2+}	Zn^{2+}	Co^{2+}	Ni^{2+}	Cu^{2+}
K_{SV}(mol^{-1}L)	58.81×10^3	-2.85×10^3	16.07×10^3	-0.159×10^3	-0.135×10^3	-0.00834×10^3	0.449×10^3

Figure S3: (A) Stern–Volmer plots of MPC-1 with the gradual addition of Co^{2+}, Ni^{2+}, Cu^{2+}, Zn^{2+}, Cd^{2+}, Hg^{2+}, and Pb^{2+}. (B) A ratiometric plot of MPC-1 for Excimer to Monomer formation (Excimer λ_{em} = 450nm/Monomer λ_{em} = 360nm) in the presence of various metal ions, utilizing an excitation wavelength of λ_{ex} = 260nm. (C) Stern–Volmer plots of monomer (**Left Axis**) and excimer (**Right axis**) formation with MPC-1 on gradual addition of Pb^{2+} ions.

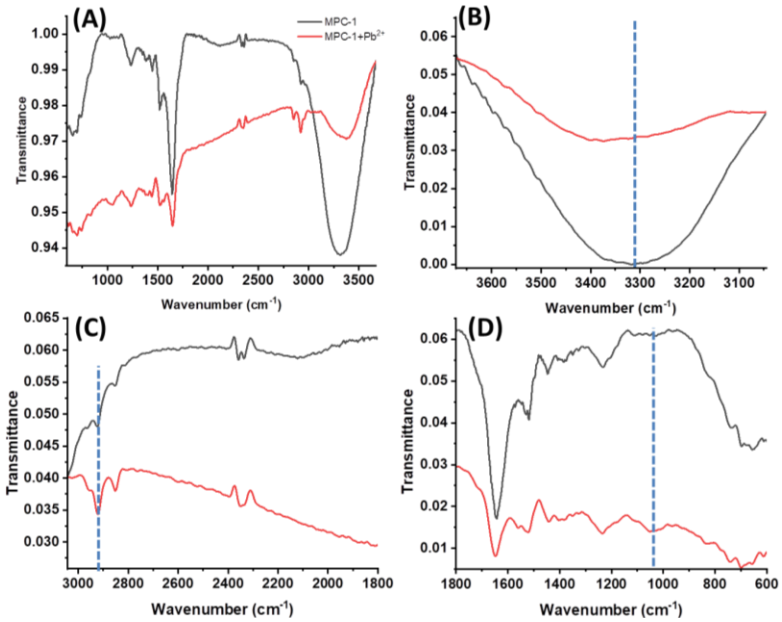

Table S4: (A) FT-IR spectra of MPC-1 alone (**Black**) and with Pb^{2+} ion (**Red**); **(B)** Amide A and B regions ranging from 3600–3000 cm^{-1}, representing N–H bond stretching; **(C)** Amide I and II regions ranging from 1800 to 1500 cm^{-1}; and **(D)** Fingerprint region ranging from 1400 to 600 cm^{-1}. These spectra depict clear differences in the free H-bonding and N–H vibrations in the amide regions A, as well as differences in the nature of H-bonding interactions after the addition of Pb^{2+} ion. Conversely, differences in the out-of-plane (Ar C–H) vibration band were observed in the fingerprint region (D) (1400 $cm^{-1}$to 600 cm^{-1}). Additionally, the amide regions I and II, which provide insights into the differences in the amide backbone, showed quit similar band positions.

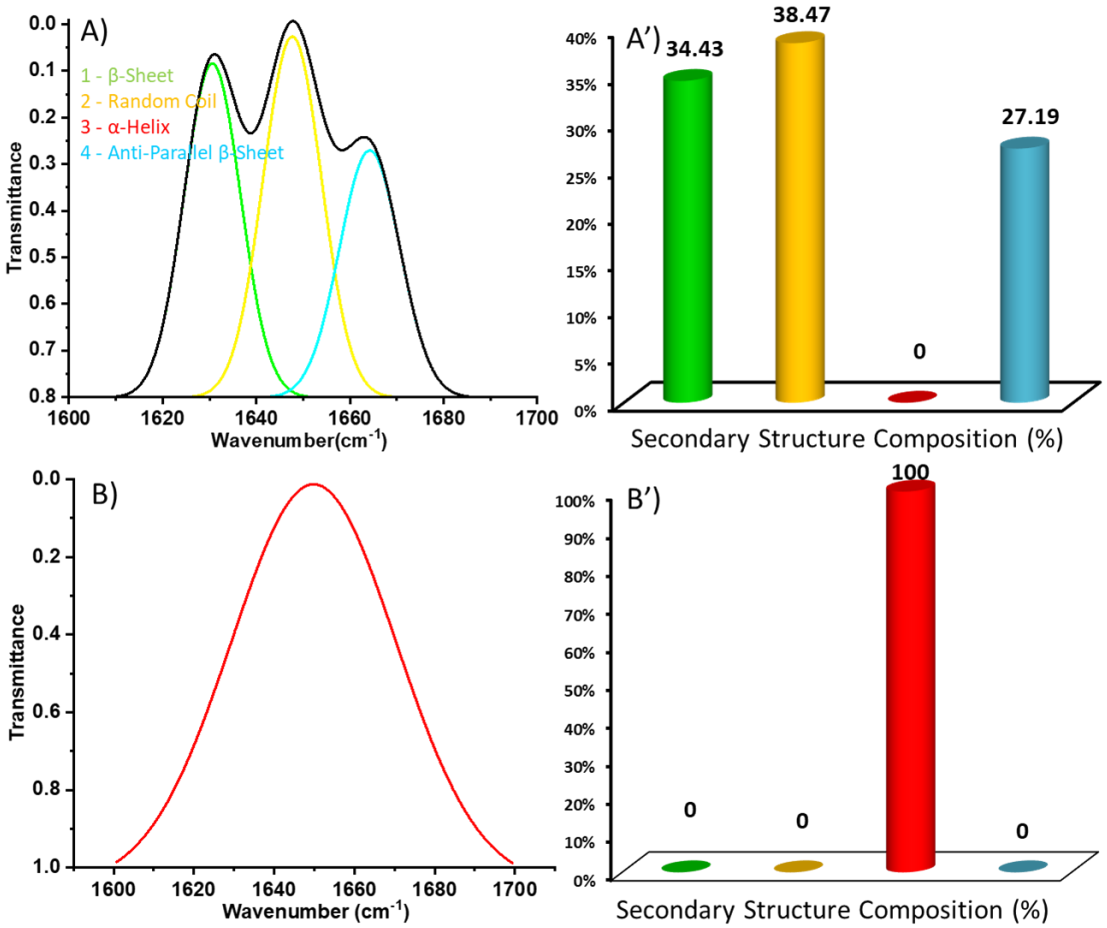

Figure S5: (A) FT-IR spectrum of MPC-1 (solid line) and its deconvolution (coloured line), A') Corresponding secondary structure contribution in self-assembly, **(B)** FT-IR spectrum of MPC-1 with lead (solid line) and its deconvolution (dashed line), B') Corresponding secondary structure contribution in self-assembly. Deconvolution was done using multiple Gaussian peaks fit in the amide I region, ranging from 1,600 to 1,700 cm^{-1}.

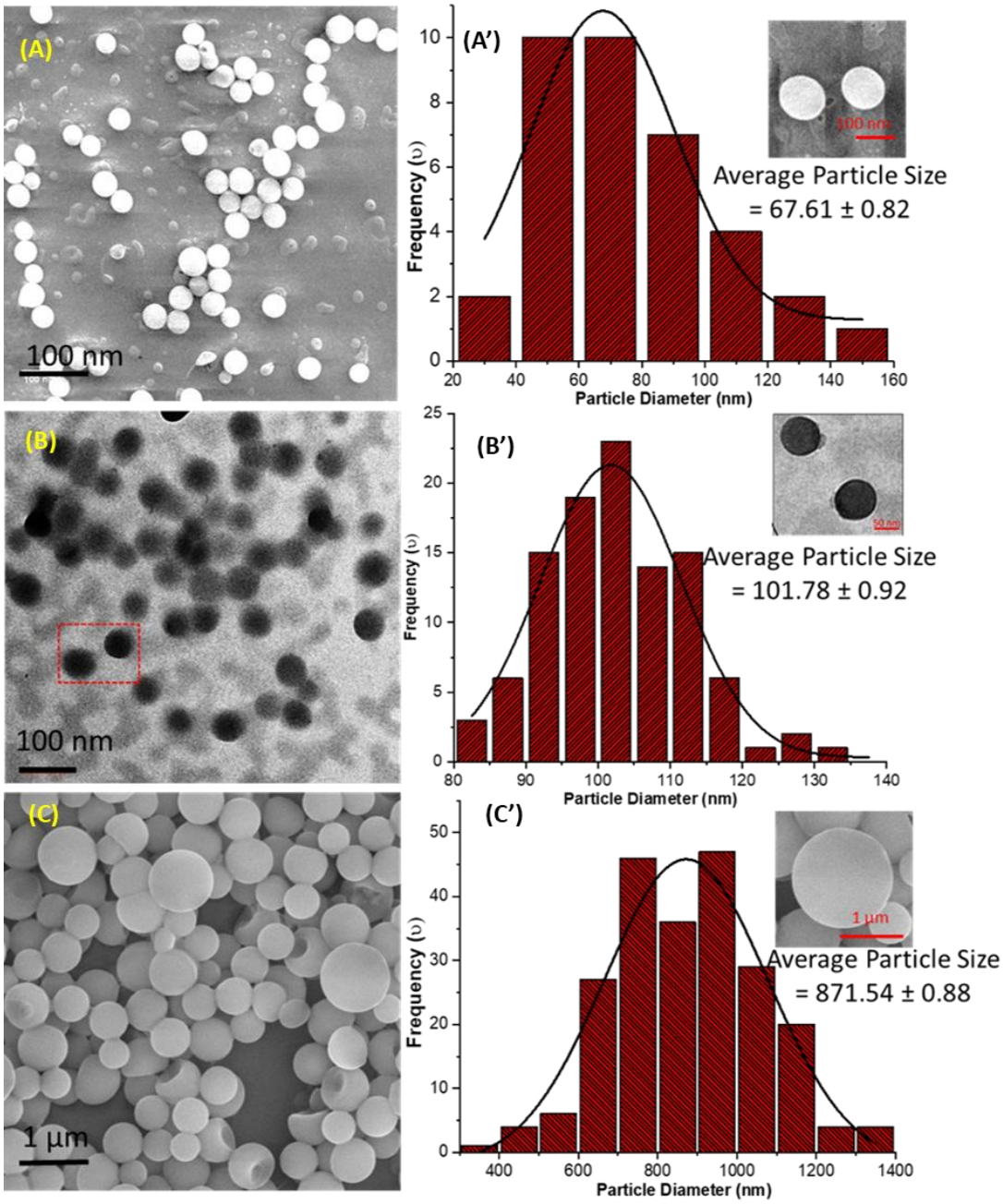

Figure S6: Quantitative morphological analysis of MPC-1 before and after the addition of Pb^{2+} ions **(A)** SEM images of MPC-1 showing nanovesicle-like self-assembly and (A′) its corresponding particle (diameter of vesicles) size distribution histogram suggest the average size of particles around 67 nm which is well corresponded with **(C)** TEM images of MPC-1 and (C′) represent its particle size distribution histogram depict the average particles size around 101 nm, (D)& (D′) shows SEM image and its particle size distribution after the addition of Pb^{2+} ions suggest the unusual enlargement of vesicles size from 100 nm to 871 nm and aggregation behaviour might be due to encapsulation or complexation of pb^{2+} ions into nanovesicles.

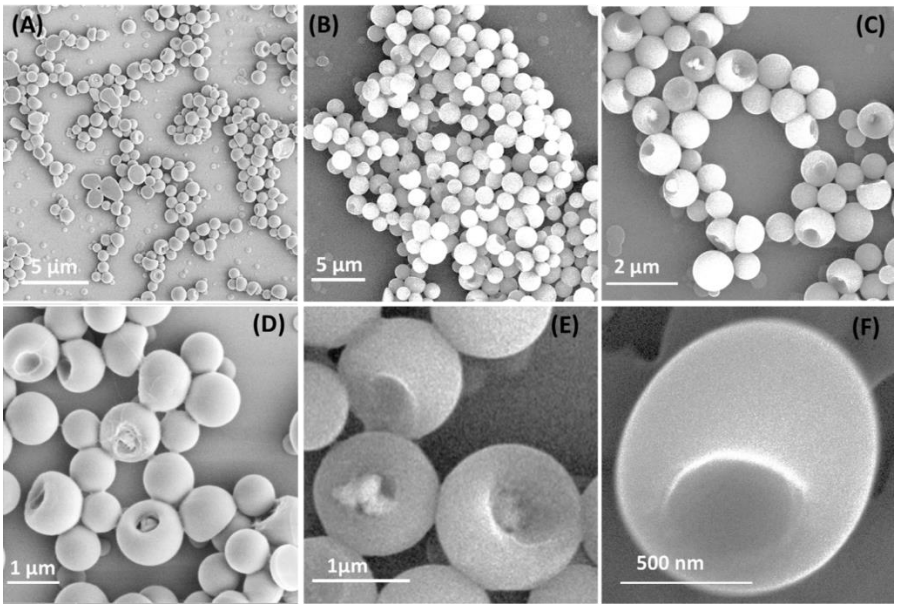

Figure S7: Insight into the Morphological Characteristics of the MPC1-Pb^{2+} Complex via SEM Analysis. Detailed SEM images delineating the hierarchical assembly of coagulated spherical/pot-like structures, indicative of peptide-mediated self-assembly processes nano-manipulated by Pb^{2+} ions. Notably, an ordered arrangement is observed, with a distinct inner view highlighting the cohesive chain-like structures of MPC1-Pb complexes. Further SEM observations reveal the intricate pot-like architecture filled with internal material, underscoring the complexity and organization inherent in peptide-driven assembly mechanisms.

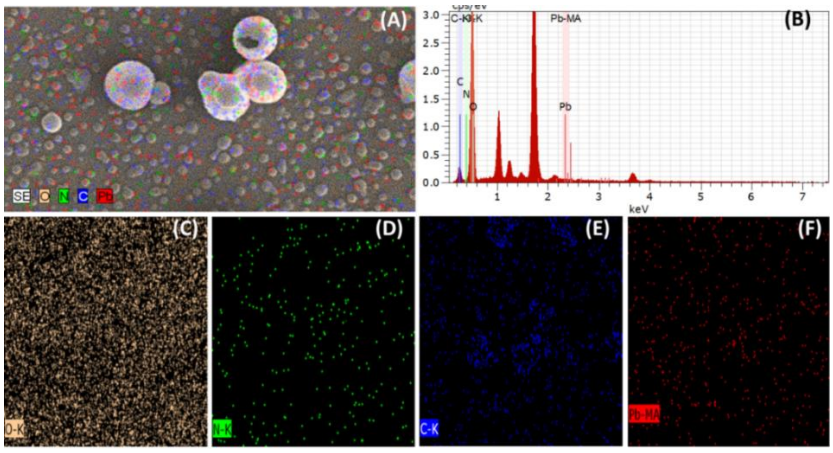

Figure S8: Characterization of self-assembled structures through EDS and colour mapping analysis of SEM images. The elemental composition revealed by EDS indicates the presence of core components such as Oxygen, Nitrogen, and Carbon from the MPC molecule. Additionally, the structures exhibit regions highlighted in red, indicative of the presence of Pb^{2+} ions. This observation directly correlates with the nanomanipulated embedding of lead within MPC-1 self-assembled vesicles.

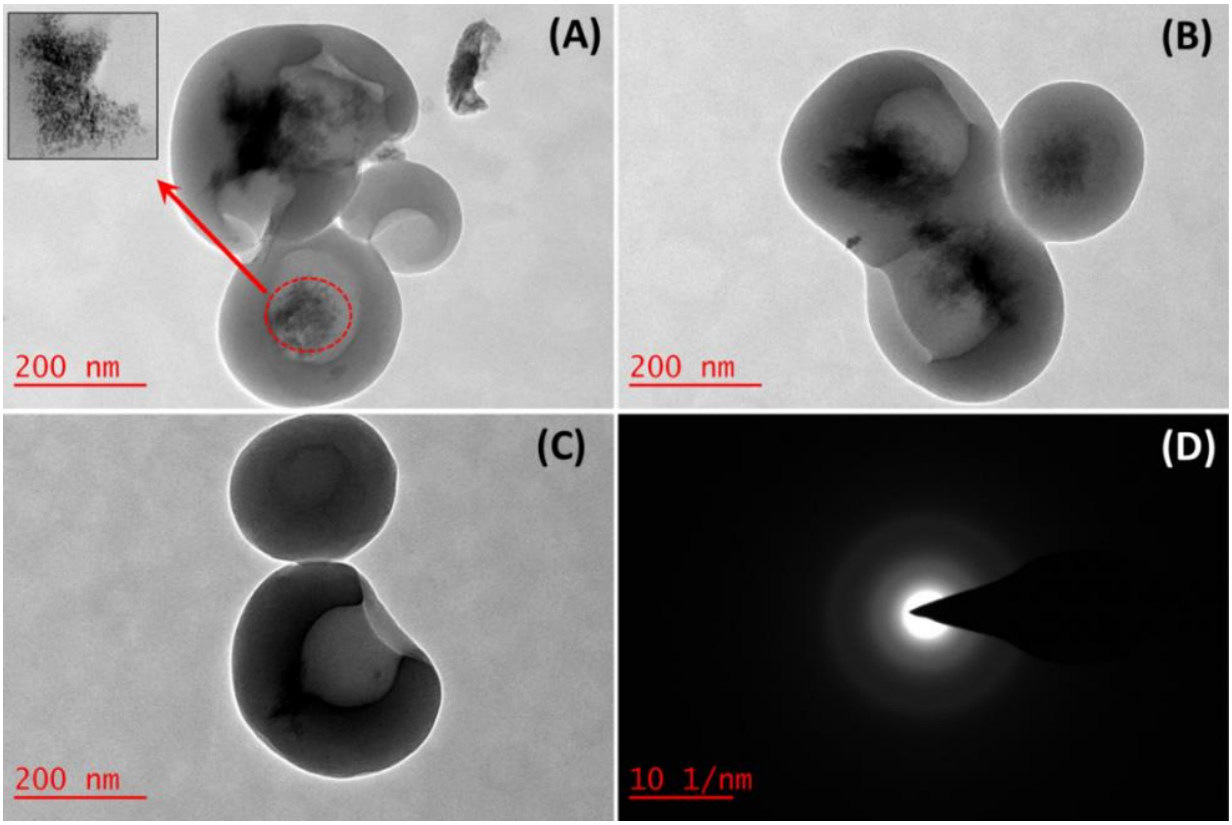

Figure S9: TEM image analysis unveils the intricate self-assembly dynamics of MPC1-Pb^{2+} structures. (A) Highlights the pot/vesicle-like assembly, revealing the fusion of vesicles embedded by lead or the initial stages of pot-like structure formation. Notably, TEM images (B) exhibit varying colour contrasts within the soft structures, indicative of potential heavy metal ion presence, specifically lead. (D) Presents the SAED pattern of the image (B), affirming the amorphous nature of lead-embedded structures, and providing further evidence for the incorporation of lead within these assembled nanostructures.

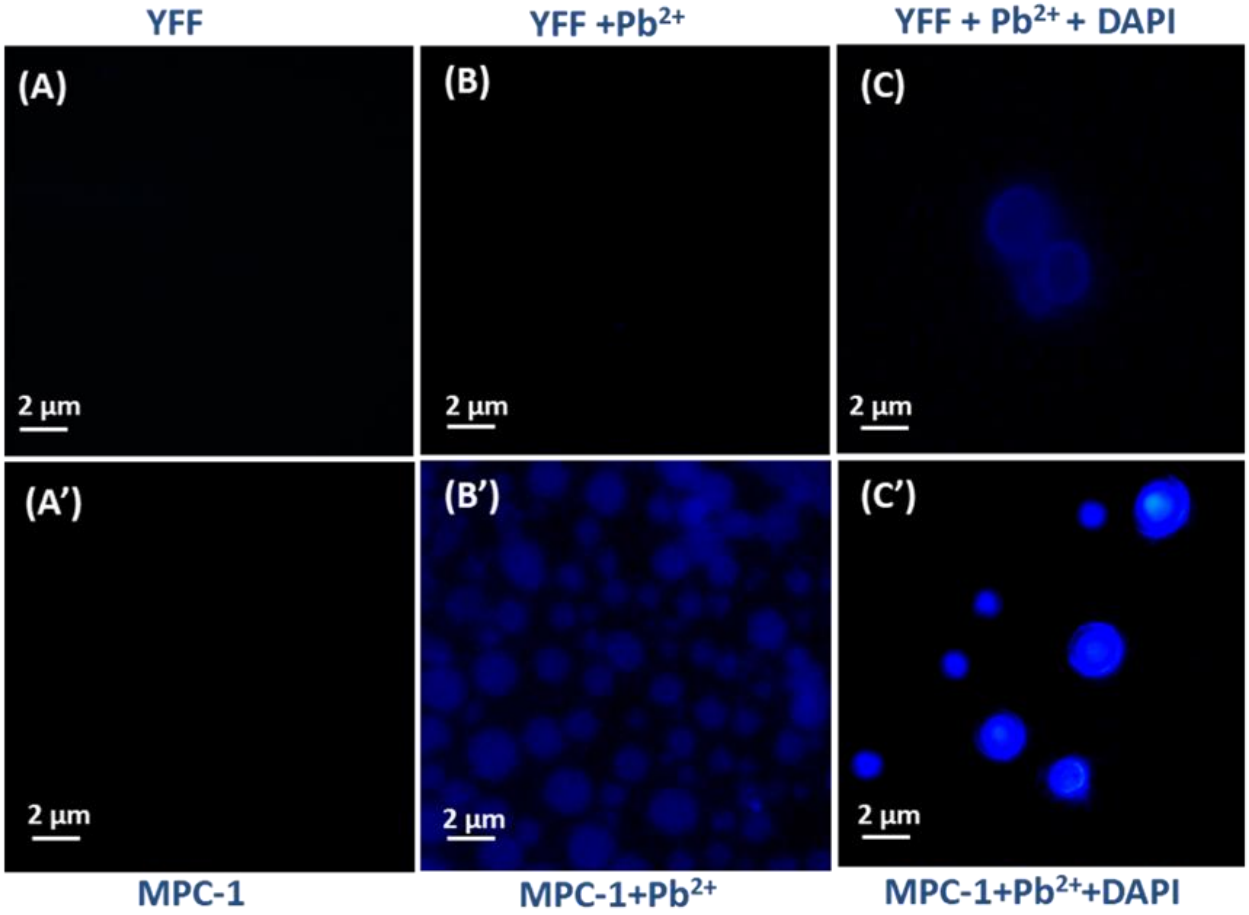

Figure S10: Fluorescence microscopy was utilized to probe the morphology of YFF and MPC-1 in the presence of Pb^{2+} ions and DAPI. Initial imaging (A) & (A′) without staining revealed no discernible morphology for either YFF or MPC1 under 358 nm excitation observed through a blue filter (λ_{em}=450nm) in the dark field, indicating the absence of inherent fluorophores necessary for proper imaging. Upon introduction of Pb^{2+} ions (B) & (B′), YFF+Pb^{2+} showed no noticeable morphological changes, whereas MPC-1&Pb^{2+} exhibited distinct blue emission, suggesting intrinsic blue light emission capability within the MPC-Pb complex. Subsequent staining with DAPI for a 12-hour incubation period resulted in minute signals for YFF-Pb complexes, while MPC1-Pb showed increased emission intensity (C) & (C′), particularly concentrated around the Pot/Sphere-like structure, potentially indicative of MPC-Pb-DAPI interactions.

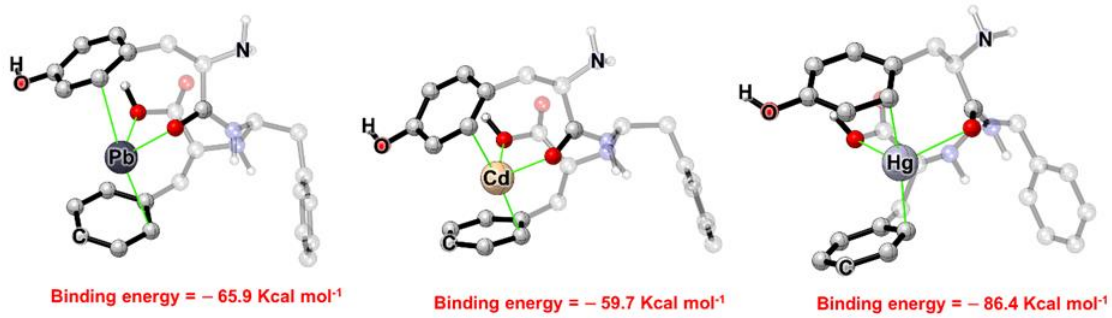

Figure S11: Depicts the active binding site of YFF's cavity and its interaction with different metals (Pb^{2+}, Cd^{2+}, Hg^{2+}) along with their binding energies.

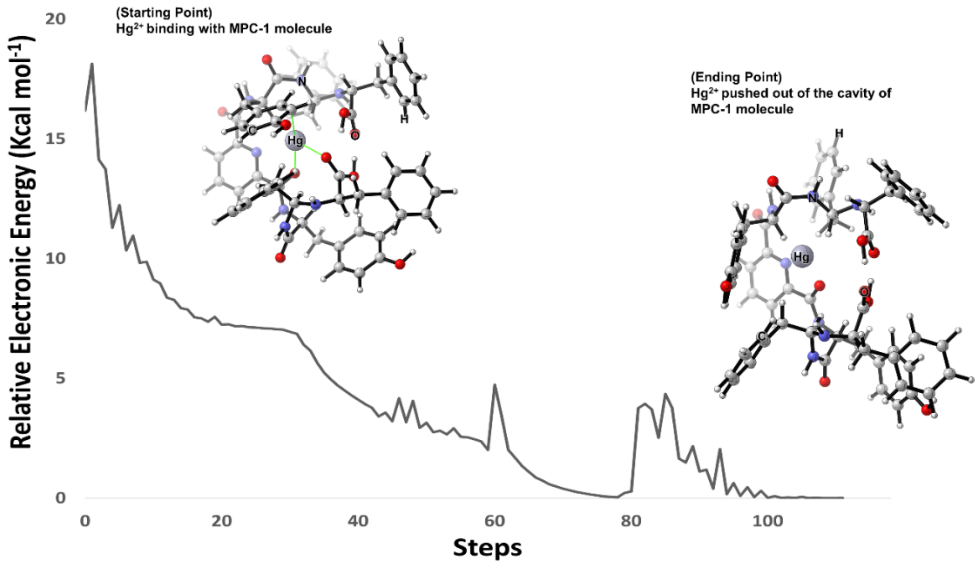

Figure S12: Energy convergence plot depicting the interaction between Hg^{2+} ions and the MPC-1 molecule. The plot illustrates the placement of Hg^{2+} within the cavity of the MPC-1 molecule, and as the convergence point approaches, it indicates the gradual release of Hg^{2+} from the cavity.

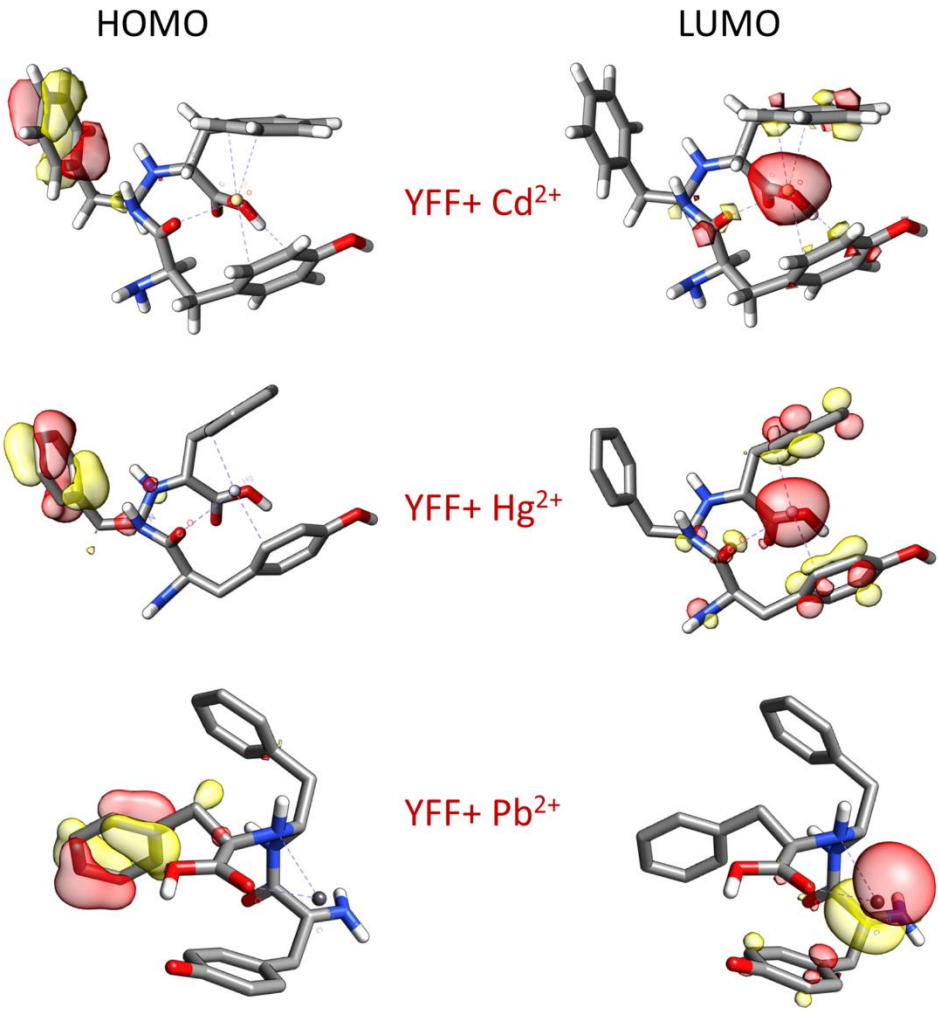

Figure S13: Computational model illustrating the optimized geometry of the YFF molecule, highlighting the configuration of its binding cavities/sites. The image depicts the interactions of Pb^{2+}, Cd^{2+}, and Hg^{2+} ions within the specified cavities.

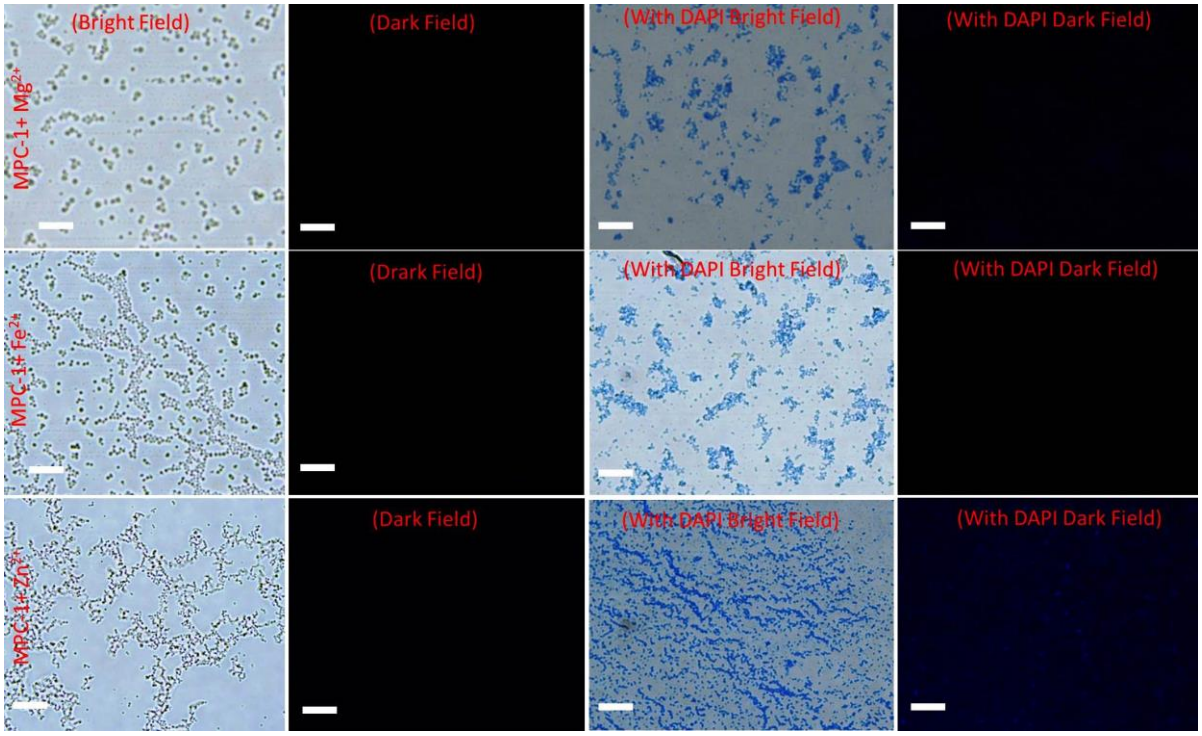

Figure S14: This figure illustrates the optical microscopy (OM) images captured in both bright field and dark field in the presence of three biologically relevant metal ions: Mg^{2+}, Fe^{2+}, and Zn^{2+}. The top panel displays OM images of MPC-1 with Mg^{2+}; the middle panel shows OM images of MPC-1 with Fe^{2+}; and the bottom panel presents OM images of MPC-1 with Zn^{2+}, both without and with DAPI. These images demonstrate the specificity of MPC-1 for lead ions in complex biological environments**.** Scale bar 5µm.

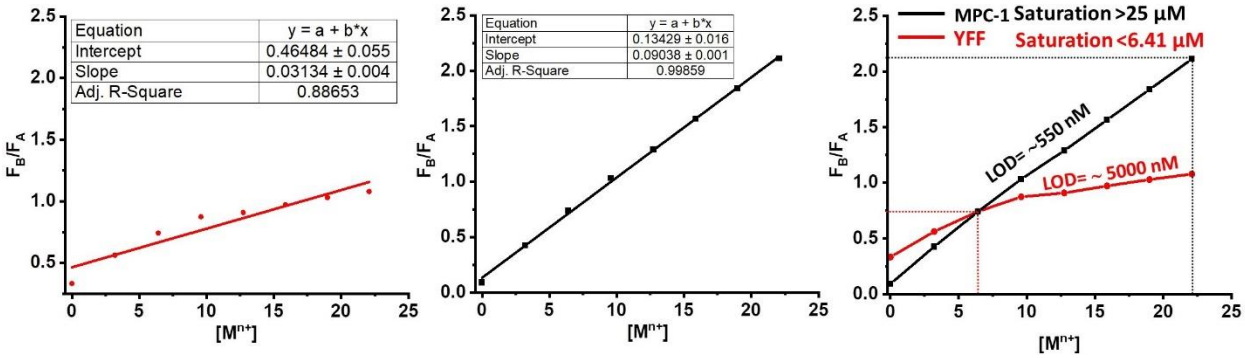

Figure S15: Ratiometric plot of (A) YFF with Pb(II) and (B) MPC-1 with Pb(II) used for calculations of LOD and LOQ which is further merged in figure (c) for better comparison.

Sl. No.	Probe	LOD	Methods/Techniques	Selectivity for Pb^{2+} tested in the presence of M^{n+} ions	Real-world Practical Applications	Reference no. in the main text
1.	Gallic acid–Au NPs	5.0 µM	Based on Ratiometric Uv-Vis Spectroscopic Absorbance	Ca^{2+}, Cu^{2+}, Cd^{2+}, Hg^{2+}, Mg^{2+}, Ni^{2+}, and Zn^{2+}	Naked-Eye Detection from Aqueous Media	67
2.	Glutathione-Capped Quantum Dots	40 nm	Based on Fluorescence Quenching of GSH-capped QDs	Na^{+}, Ba^{2+}, Ca^{2+}, Mg^{2+}, Co^{2+}, Ni^{2+} , Li^{+}, K^{+}	Not Available	68
3.	Peptide–Au NPs	242 nM	Based on Uv-Vis Spectroscopic Absorbance and Colorimetric response	No selectivity	Not Available	58
4.	2- Mercaptoethanol/S_2O_3 2–Au NPs	0.5 nM	Based on the Leaching of Gold Nanoparticles	No selectivity	Not Available	69
5.	Au NPs, DNAzyme and substrate	0.5 µM	Based on quenching and ratiometric absorbance of DNAzyme using unmodified gold nanoparticle probes	Towards (Zn^{2+} , Co^{2+}, Mg^{2+}, Ca^{2+}, Mn^{2+}, Cd^{2+}, Ni^{2+}, and Cu^{2+}	Not Available	70
6.	DNA–Au NPs, DNAzyme and substrate	0.5 µM	Based on Uv-Vis Spectroscopic Absorbance and Colorimetric response	NA/NA	Not Available	71
7.	Graphene Quantum Dots/L-Cysteine	70 nM.	Quenching of Graphene Quantum Dots/L-Cysteine Coreactant Electrochemiluminescence System	Hg^{2+}, Cu^{2+}, Co^{2+}, Fe^{3+}, Ni^{2+}, Ag^{2+} , Ca^{2+}, Cd^{2+}, Mn^{2+}, Mg^{2+}, Ba^{2+} , Na^{+}, Li^{+} and Zn^{2+}	Not Available	72
8.	1,8-naphthalimide dye with cellulose nanocrystals (CNCs)	150 nM	Fluorescence enhancement of cellulose nanocrystals CNCs	Ba^{2+}, Cu^{2+}, Zn^{2+}, Fe^{2+}, Co^{2+}, Ni^{2+}, and Mg^{2+}	Not Available	73

9.	A group of Cysteine-rich cyclic peptides	NA	Not mentioned	Zn^{2+} and Ca^{2+}	Detoxification in bacterial (DH5a cells) and human cell culture (HT-29 cells)	8
10.	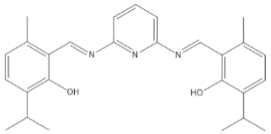	0.49 µM	Based on the fluorescent enhancement response	Cr^{3+}, Mn^{2+} , Fe^{3+}, , Co^{2+} , Ni^{2+} , $Cu2^{2+}$, Zn^{2+} , Hg^{2+} , Bi^{3+}, Ag+, Cd^{2+} , Th^{4+} , Ce^{4+} , Nd^{3+}, and U^{6+}	Not Available	74
11..	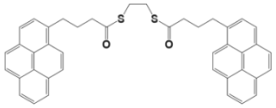	NA	Based on Ratiometric Fluorescence Spectroscopic response.	K^{+}, Na^{+}, Ag^{+}, Ba^{2+}, Ca^{2+}, Cd^{2+}, Co^{2+}, Cu^{2+}, Fe^{2+}, Hg^{2+}, Mg^{2+}	Not Available	75
12.	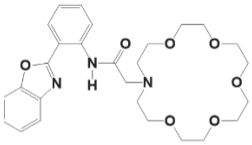	160 nM	Based on the excited state intramolecular proton transfer (ESIPT)	Fe^{2+}, Co^{2+}, Ni^{2+},Cu^{2+}, Zn^{2+}, Cd^{2+}, Hg^{2+}, Mg etc	Not Available	76
13.	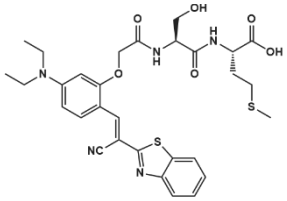	6.3 nM	Based on the Ratiometric fluorescent detection	Fe^{2+}, Co^{2+}, Ni^{2+}, Cu^{2+}, Zn^{2+}, Cd^{2+}, Hg^{2+}, Mg+, Mn^{2+} etc.	Ratiometric detection of Pb^{2+} in tap water, groundwater, and live cell.	77
14.	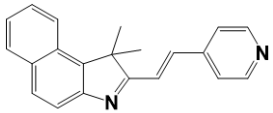	3.4 µM	Based on ratiometric fluorescent response.	K^{+}, Na^{+}, Ca^{2+}, Ag+, Mg^{2+}, Hg^{2+}, Co^{2+}, Fe^{2+}, Mn^{2+}, Pd^{2+}, Cd^{2+}, Ni^{2+}, Zn^{2+}	Cu^{2+} and Pb^{2+} were detected in a test strip	78
15.	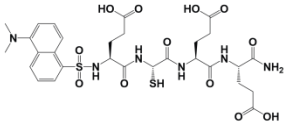	NA	Based on Ratiometric Fluorescence Spectroscopic response.	Ca $^{2+}$, Cd^{2+}, or Zn^{2+}	Not Available	79

16.	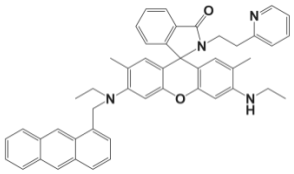	210 nM	Based on chromogenic and fluorogenic 'turn-on' spectral responses	Mn^{2+}, Fe^{2+}, Co^{2+}, Ni^{2+}, Cu^{2+}, Zn^{2+}, Cd^{2+},Hg^{2+}, Ag^{+} etc	Not Available	80
17.	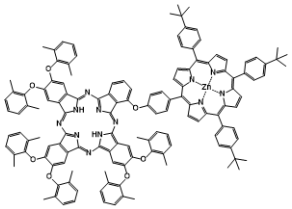	3.4 nM	Based on the Ratiometric response of Intermolecular fluorescence resonance energy transfer (FRET) processes from the porphyrin donor to the phthalocyanine acceptor.	Ag^{+}, Al^{3+}, Ba^{2+}, Ca^{2+}, Cd^{2+}, Co^{2+}, Cr^{3+}, Cu^{2+}, Fe^{2+}, Fe^{3+}, Hg^{2+}, K^{+}, Mg^{2+}, Mn^{2+}, Na^{+}, , NH^{4+}, Ni^{2+}, and Zn^{2+}	Not Available	81
18.	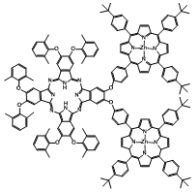	4.1 nM	Based on the Ratiometric response of intramolecular fluorescence resonance energy transfer (FRET) process	Ag^{+}, Al^{3+}, Ba^{2+}, Ca^{2+}, Co^{2+}, Cr^{3+}, Cu^{2+}, Fe^{2+}, Fe^{3+}, K^{+}, Mg^{2+}, Mn^{2+}, Na^{+}, NH_4^{+} and Ni^{2+}	Not Available	82
19.	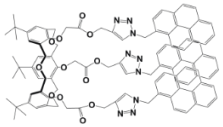	NA	Enhancement of the monomer emission of pyrene	Ag^{+}, Co^{2+}, Ni^{2+}, Hg^{2+}, Zn^{2+}, Cd^{2+}, Cu^{2+}	Not Available	83
20.	Pyridine-bis-YFF peptide conjugate	~550 nM	Based on Ratiometric Monomer-Excimer formation	Fe^{2+},Co^{2+}, Ni^{2+}, Cu^{2+}, Zn^{2+}, Cd^{2+}, Hg^{2+}, Mg^{2+}	In vivo detoxification in RPE-1 cell lines	**Current work**

Table S1: Offers a detailed review of current technologies, encompassing their detection limits, selectivity, and practical applications. This comprehensive assessment highlights the novelty and superiority of our proposed metallopeptide nanoreservoirs.

15.0 Cartesian coordinates for the optimized Geometries

DFT optimization method: BP86-D3/def-SVP

MPC-1 molecule

C	10.882182618014	-6.935027692862	18.684288341374
H	11.073546942116	-7.942547205117	19.092886865569
C	12.148703999771	-6.294105151120	18.068177119744
O	12.029912760435	-5.289971051468	17.360088154782
C	10.345777257789	-6.030880571280	19.818032700603
H	10.132866062743	-5.026640202713	19.395692368652
H	9.388071226404	-6.460566798872	20.176332880251
C	11.350827440181	-5.929817186414	20.943676160511
C	11.405106629101	-6.909977424762	21.954993971828
C	12.331091959928	-4.914149729648	20.951163637284
C	12.396724202485	-6.879741975665	22.946536676377
C	13.325698989496	-4.869102374473	21.934099873958
C	13.365495080197	-5.856159060540	22.939838669240
H	10.661952705848	-7.723176600133	21.967874038622
H	12.318056069725	-4.149527756327	20.158917445017
H	12.428780253013	-7.663995653829	23.719272916888
H	14.091987974364	-4.080700617998	21.936554019379
O	14.366392532952	-5.779386500441	23.864576652545
H	14.358199319999	-6.585708091359	24.417726334729
N	13.345854707396	-6.870204626197	18.366024215502
C	13.569744537423	-8.087078620762	19.159048853633
N	14.926085399296	-8.062740008383	19.693385568037
C	15.067546307489	-8.511180101454	21.080624918250
C	14.435795940250	-9.900598357304	21.217848461189
O	13.240041332942	-9.906819822181	21.756643273159
O	14.978287973274	-10.910098273605	20.715645385852
H	12.756193003935	-10.819965058683	21.592331846459
C	13.254640305226	-9.367206657756	18.332266033084
C	14.848136280452	-9.179686580085	14.861252916998
C	16.027720161393	-9.921725821381	15.046246146103
C	13.947397947589	-9.009331557558	15.923336164431
H	16.729218905348	-10.061715877285	14.209860901497
H	13.018038456934	-8.438816454598	15.772773201694
C	16.300381896639	-10.493445545134	16.299329533521
C	14.207853449944	-9.579811816721	17.187479183105
H	17.216067169253	-11.085748134059	16.449072914997
C	15.398469093414	-10.322017520584	17.363015663213

H	15.603095635141	-10.787148505314	18.340594003680
H	14.624896322311	-8.736957717154	13.878441901805
C	16.540831311472	-8.523645226542	21.515298458988
C	16.717860278536	-7.811227509179	23.943296669075
C	16.670346905912	-8.848282356679	22.987810364758
C	16.747607473454	-8.100884504743	25.317894741241
H	16.796484404130	-7.278609926223	26.049101055296
C	16.667910155586	-10.184891595117	23.440883790136
C	16.731746553272	-9.435839781272	25.758274519147
H	16.637132180476	-11.004116802660	22.706492514287
H	16.757758255710	-9.664380240906	26.834650514112
C	16.696995923078	-10.475655094744	24.814812242522
H	16.695928154674	-11.524209938505	25.150517992060
H	16.723553814647	-6.764479177501	23.603533326531
H	12.877216924901	-8.050825720775	20.023333417914
H	16.961141386644	-7.523931209056	21.288861301618
H	17.084469185667	-9.271534572125	20.900378384308
H	12.210271227282	-9.318354232238	17.966779100794
H	13.288074684806	-10.235600602134	19.013646072599
H	14.176101249832	-6.408989423095	17.982665373478
H	14.493305327747	-7.820409382261	21.728518117441
H	15.561671897215	-8.591139862505	19.076832369458
N	9.905183736420	-7.135247095511	17.628534728881
H	9.568007992500	-6.300753670469	17.143929261275
C	8.020376403658	-12.470408348998	16.155968349796
H	8.406244079364	-11.614546395005	16.734468181796
C	7.787308996254	-13.721283764186	17.026559999675
O	6.982952888448	-14.580843282738	16.642651084225
C	9.035010171985	-12.786033403081	15.015237662897
H	8.593089149885	-13.580852465809	14.380241014578
H	9.121539142639	-11.868766492646	14.396502109373
C	10.385458809742	-13.207883331386	15.536103560255
C	11.323101612216	-12.253978228498	15.986830365681
C	10.702358237519	-14.573903422905	15.688693830225
C	12.523688957438	-12.648794650401	16.593868967957
C	11.894371214982	-14.982090451731	16.300206510597
C	12.805187295219	-14.018596671970	16.778774891290
H	11.094018064239	-11.180245830399	15.902982421687
H	9.979809681388	-15.333181085701	15.350269745299
H	13.247055759861	-11.895424085912	16.934230679840
H	12.126195871523	-16.047834806912	16.443365015755
O	13.917666455085	-14.455220255792	17.442508295572
H	14.157796486995	-13.772658002470	18.107583364764

N	8.474825430834	-13.851774000783	18.193015746734
C	9.497943447215	-13.008510605552	18.850835872115
N	10.083222033850	-13.830501348570	19.898286887196
C	11.509200212690	-14.044840952428	19.919549325132
C	12.340132523187	-12.823385701928	20.318934794790
O	13.510492089897	-12.718135673076	19.714178526653
O	11.948856787126	-12.031699097310	21.196308252296
H	14.116003576733	-11.998286514816	20.181147462194
C	8.923315932840	-11.676917718837	19.407291198103
C	5.650339563824	-12.440150186445	21.236516894103
C	6.069728855481	-12.447721127429	22.578739918726
C	6.567155323730	-12.163735525111	20.211049286158
H	5.348684413934	-12.664202102100	23.381899862531
H	6.233552616963	-12.153218973267	19.161972374239
C	7.410574391252	-12.169582575453	22.889576902641
C	7.919548332388	-11.888776470492	20.509107245771
H	7.744551388030	-12.163887202444	23.938887493138
C	8.328194637256	-11.891749076323	21.861738955346
H	9.380260358505	-11.666755039225	22.102028562306
H	4.598946565084	-12.650264679247	20.986573448021
C	11.848732335744	-15.182519545451	20.932856459717
C	14.194141577079	-15.928295242739	20.304392270862
C	13.326532501663	-15.303000065700	21.223013332162
C	15.580643537309	-15.929545689971	20.518921715489
H	16.244186387692	-16.416506950593	19.787993733131
C	13.879149039366	-14.686630073118	22.364734315969
C	16.122293191916	-15.303819103025	21.655286700471
H	13.210342498805	-14.190246764388	23.085930896223
H	17.210659393773	-15.302245919268	21.820036202228
C	15.266667349847	-14.684014039270	22.580568787212
H	15.680477570579	-14.196367709759	23.476705496551
H	13.783228996090	-16.389673868965	19.394032231088
H	10.274884681712	-12.750222068827	18.103700186431
H	11.430493922548	-16.118270478597	20.511706912102
H	11.298358028281	-14.965763806836	21.872640599646
H	8.485316863817	-11.094531217399	18.574353718933
H	9.785370183064	-11.085298384118	19.771652169556
H	8.304868519250	-14.733471728961	18.686312257454
H	11.845162302353	-14.356988570934	18.913053790480
H	9.712965448240	-13.583451137800	20.824853682646
N	6.703490378119	-12.144994793897	15.612376977492
H	6.117748756609	-12.987369983047	15.505376526078
C	7.586776733073	-7.623920686613	13.980386255104

C	6.852217084985	-8.814125878363	13.937018364682
C	7.097565392490	-9.790706032051	14.927278945393
N	7.980079100222	-9.603373888483	15.916934748628
C	8.663358854229	-8.449120621743	15.979120637655
C	8.512493092971	-7.428206153911	15.020165771164
H	7.446635382192	-6.850452975478	13.210026798110
H	6.094736042465	-9.023747971170	13.169068752839
H	9.121631316322	-6.511786610517	15.059201495915
O	5.234345849833	-11.088339540590	14.222558579684
C	6.278373499666	-11.069514263927	14.883773759022
O	10.125001553766	-9.413733971110	17.608960974701
C	9.634576000496	-8.380254090542	17.135441666241

MPC-1 molecule + Pb^{2+}

C	11.409256000000	-6.721021000000	19.018088000000
H	11.798261000000	-7.642769000000	19.478663000000
C	12.446393000000	-6.019331000000	18.084019000000
O	12.224034000000	-4.875946000000	17.702315000000
C	11.012935000000	-5.764530000000	20.158266000000
H	10.745826000000	-4.778970000000	19.726755000000
H	10.124734000000	-6.179728000000	20.676171000000
C	12.187844000000	-5.656968000000	21.107095000000
C	12.350919000000	-6.596977000000	22.144906000000
C	13.201414000000	-4.692334000000	20.912693000000
C	13.483145000000	-6.581809000000	22.970928000000
C	14.332054000000	-4.657069000000	21.735150000000
C	14.478958000000	-5.599521000000	22.776529000000
H	11.576625000000	-7.360464000000	22.319018000000
H	13.096159000000	-3.949601000000	20.107250000000
H	13.593717000000	-7.323844000000	23.777323000000
H	15.111292000000	-3.893354000000	21.600353000000
O	15.585107000000	-5.512329000000	23.555415000000
H	15.568162000000	-6.237932000000	24.212159000000
N	13.556446000000	-6.731575000000	17.712366000000
C	13.856774000000	-8.130273000000	17.993734000000
N	15.028043000000	-8.320225000000	18.811683000000
C	14.810138000000	-8.687370000000	20.194767000000
C	13.751809000000	-9.779257000000	20.328200000000
O	12.932772000000	-9.660707000000	21.330489000000
O	13.681081000000	-10.738408000000	19.497503000000
H	12.315182000000	-10.490517000000	21.385314000000

C	13.892122000000	-8.991807000000	16.711042000000
C	16.257349000000	-7.780110000000	13.952400000000
C	17.390862000000	-8.579313000000	14.180486000000
C	15.117853000000	-7.918103000000	14.761891000000
H	18.279177000000	-8.471856000000	13.540888000000
H	14.230628000000	-7.294170000000	14.568677000000
C	17.385078000000	-9.518115000000	15.225347000000
C	15.097939000000	-8.854285000000	15.817132000000
H	18.269969000000	-10.145445000000	15.409956000000
C	16.245498000000	-9.654744000000	16.038666000000
H	16.251728000000	-10.384513000000	16.866978000000
H	16.258777000000	-7.045996000000	13.132883000000
C	16.139523000000	-9.196063000000	20.823777000000
C	16.702770000000	-8.353402000000	23.139702000000
C	16.108818000000	-9.339826000000	22.327599000000
C	16.653091000000	-8.451334000000	24.541064000000
H	17.159687000000	-7.695374000000	25.162486000000
C	15.482484000000	-10.440205000000	22.950844000000
C	15.991774000000	-9.530847000000	25.150759000000
H	15.060534000000	-11.255527000000	22.340382000000
H	15.951411000000	-9.608673000000	26.247337000000
C	15.410216000000	-10.528154000000	24.349619000000
H	14.911090000000	-11.387057000000	24.823432000000
H	17.212710000000	-7.497823000000	22.671610000000
H	12.965666000000	-8.504150000000	18.530029000000
H	16.907225000000	-8.452477000000	20.529250000000
H	16.404160000000	-10.158805000000	20.333854000000
H	12.964774000000	-8.778562000000	16.140811000000
H	13.850302000000	-10.044893000000	17.069106000000
H	14.247622000000	-6.191593000000	17.178172000000
H	14.448721000000	-7.817870000000	20.787461000000
H	15.775937000000	-8.846304000000	18.351441000000
N	10.284964000000	-7.142769000000	18.175980000000
H	9.664987000000	-6.405806000000	17.824118000000
C	8.617984000000	-12.967843000000	16.659155000000
H	9.077950000000	-12.115572000000	17.205163000000
C	8.751429000000	-14.292947000000	17.452517000000
O	8.732273000000	-15.365200000000	16.852121000000
C	9.291249000000	-13.102321000000	15.269662000000
H	9.019355000000	-14.101090000000	14.870937000000
H	8.867947000000	-12.332114000000	14.597580000000
C	10.783967000000	-12.940157000000	15.350334000000
C	11.408233000000	-11.756247000000	14.875167000000

C	11.617819000000	-13.929190000000	15.946759000000
C	12.801186000000	-11.557779000000	14.986214000000
C	13.001156000000	-13.733838000000	16.087505000000
C	13.618482000000	-12.549326000000	15.595848000000
H	10.796908000000	-10.983652000000	14.382622000000
H	11.164910000000	-14.872602000000	16.289041000000
H	13.268165000000	-10.655357000000	14.562921000000
H	13.639305000000	-14.504744000000	16.543837000000
O	14.943552000000	-12.428230000000	15.739743000000
H	15.275935000000	-11.565659000000	15.390477000000
N	8.818547000000	-14.229018000000	18.817724000000
C	8.955258000000	-13.094682000000	19.733638000000
N	9.385970000000	-13.624297000000	20.989323000000
C	10.765649000000	-14.042698000000	21.123162000000
C	11.697630000000	-12.852234000000	20.913105000000
O	12.734760000000	-13.080203000000	20.108014000000
O	11.448343000000	-11.747595000000	21.416717000000
H	13.283329000000	-12.223708000000	20.029724000000
C	7.703159000000	-12.200965000000	19.894291000000
C	4.751140000000	-14.539938000000	20.581563000000
C	4.540343000000	-14.331167000000	21.955387000000
C	5.759227000000	-13.833057000000	19.909262000000
H	3.746790000000	-14.882402000000	22.481297000000
H	5.906910000000	-13.988873000000	18.830339000000
C	5.334190000000	-13.404610000000	22.651000000000
C	6.570861000000	-12.909205000000	20.600029000000
H	5.160202000000	-13.222985000000	23.722092000000
C	6.343199000000	-12.699269000000	21.976041000000
H	6.946124000000	-11.955227000000	22.523855000000
H	4.119214000000	-15.251338000000	20.029220000000
C	11.053553000000	-14.649589000000	22.519892000000
C	13.087565000000	-16.122832000000	22.161402000000
C	12.528682000000	-14.942451000000	22.691651000000
C	14.469585000000	-16.355324000000	22.234535000000
H	14.889892000000	-17.288908000000	21.831421000000
C	13.382252000000	-13.996632000000	23.298781000000
C	15.313087000000	-15.404645000000	22.834055000000
H	12.954947000000	-13.079396000000	23.736679000000
H	16.395448000000	-15.590422000000	22.900231000000
C	14.766598000000	-14.226855000000	23.369541000000
H	15.423789000000	-13.493116000000	23.859862000000
H	12.430851000000	-16.877274000000	21.698555000000
H	9.760063000000	-12.402842000000	19.271061000000

H	10.432750000000	-15.562211000000	22.619027000000
H	10.710698000000	-13.924971000000	23.288182000000
H	7.398900000000	-11.855845000000	18.888536000000
H	8.020548000000	-11.301420000000	20.461977000000
H	8.714327000000	-15.136681000000	19.286130000000
H	11.011616000000	-14.795858000000	20.346132000000
H	9.049546000000	-13.076302000000	21.788053000000
N	7.197639000000	-12.675372000000	16.571955000000
H	6.561130000000	-13.478232000000	16.487214000000
C	7.473098000000	-7.991173000000	15.063464000000
C	6.878109000000	-9.252335000000	15.146959000000
C	7.414462000000	-10.210208000000	16.040189000000
N	8.469535000000	-9.948546000000	16.838051000000
C	8.982979000000	-8.696539000000	16.816501000000
C	8.539051000000	-7.697119000000	15.926167000000
H	7.105898000000	-7.239231000000	14.349644000000
H	5.998155000000	-9.526742000000	14.548769000000
H	9.027129000000	-6.712046000000	15.878943000000
O	5.430468000000	-11.475342000000	15.804858000000
C	6.613162000000	-11.509165000000	16.125018000000
O	10.808894000000	-9.334531000000	18.286956000000
C	10.075939000000	-8.409118000000	17.799584000000
Pb	11.612738000000	-11.450480000000	17.821808000000

YFF molecule

C	-3.096373000000	-1.792173000000	1.898545000000
H	-4.093559000000	-1.448818000000	2.241613000000
C	-2.573660000000	-2.963327000000	2.766865000000
O	-1.607338000000	-3.618809000000	2.359423000000
C	-2.119486000000	-0.595728000000	2.024495000000
H	-1.118352000000	-0.936900000000	1.688186000000
H	-2.465408000000	0.182300000000	1.314372000000
C	-2.059399000000	-0.076746000000	3.439550000000
C	-3.061537000000	0.786520000000	3.930158000000
C	-1.089190000000	-0.544735000000	4.350049000000
C	-3.123073000000	1.140400000000	5.285478000000
C	-1.135483000000	-0.198541000000	5.706652000000
C	-2.171448000000	0.625361000000	6.191059000000
H	-3.823052000000	1.179503000000	3.236776000000
H	-0.302347000000	-1.226136000000	3.990687000000
H	-3.918746000000	1.805119000000	5.653651000000

H	-0.393890000000	-0.587800000000	6.419726000000
O	-2.230914000000	0.866654000000	7.535092000000
H	-3.175544000000	0.972434000000	7.783164000000
N	-3.192614000000	-3.261274000000	3.949259000000
C	-4.247989000000	-2.542230000000	4.688273000000
N	-4.191063000000	-3.000681000000	6.066448000000
C	-4.103892000000	-2.025000000000	7.128218000000
C	-5.342037000000	-1.124821000000	7.244754000000
O	-5.039528000000	0.145324000000	7.653748000000
O	-6.490194000000	-1.469538000000	7.034459000000
H	-5.900321000000	0.605641000000	7.778127000000
C	-5.658796000000	-2.755637000000	4.061319000000
C	-6.134387000000	-6.525035000000	3.579076000000
C	-6.953253000000	-6.847813000000	4.675477000000
C	-5.738248000000	-5.196733000000	3.360648000000
H	-7.264330000000	-7.890098000000	4.844634000000
H	-5.094093000000	-4.949711000000	2.502797000000
C	-7.377092000000	-5.833334000000	5.549005000000
C	-6.156740000000	-4.168162000000	4.231965000000
H	-8.024698000000	-6.077214000000	6.405418000000
C	-6.981053000000	-4.502653000000	5.330027000000
H	-7.309142000000	-3.701634000000	6.011747000000
H	-5.801818000000	-7.315102000000	2.888246000000
C	-3.905675000000	-2.764710000000	8.481297000000
C	-2.742781000000	-1.078755000000	9.977851000000
C	-3.886996000000	-1.846683000000	9.680159000000
C	-2.751781000000	-0.165036000000	11.042464000000
H	-1.850806000000	0.429507000000	11.257601000000
C	-5.039141000000	-1.681836000000	10.475765000000
C	-3.906396000000	-0.006783000000	11.828453000000
H	-5.939879000000	-2.275222000000	10.249975000000
H	-3.912142000000	0.708540000000	12.665151000000
C	-5.050544000000	-0.770309000000	11.544122000000
H	-5.957084000000	-0.657633000000	12.158713000000
H	-1.841495000000	-1.182089000000	9.355615000000
H	-4.017676000000	-1.456242000000	4.659178000000
H	-2.958701000000	-3.333356000000	8.387396000000
H	-4.726499000000	-3.506195000000	8.585339000000
H	-5.614251000000	-2.487167000000	2.986985000000
H	-6.351305000000	-2.045535000000	4.554240000000
H	-2.755323000000	-4.016613000000	4.486150000000
H	-3.225844000000	-1.374396000000	6.954775000000
H	-4.919670000000	-3.702462000000	6.253445000000

N	-3.205526000000	-2.192930000000	0.494781000000
H	-3.963227000000	-2.884170000000	0.401306000000
H	-2.343968000000	-2.721808000000	0.280418000000

YFF molecule + Pb^{2+}

C	-3.573231348781	-0.974476675882	3.078453061435
H	-4.351352577125	-0.329266792869	3.551125172304
C	-3.346540573274	-2.132698115971	4.064512903884
O	-2.257113798274	-2.230552636720	4.730666238230
C	-2.298141811785	-0.087180479855	2.917051437350
H	-1.431691559848	-0.722288353340	2.647205060312
H	-2.496204905928	0.579884674545	2.053759189270
C	-1.989825177321	0.749108507673	4.138005974082
C	-2.816175437859	1.841730127175	4.495473013198
C	-0.905995618705	0.455582611042	4.995532822111
C	-2.625725141879	2.565884937057	5.688886710031
C	-0.703780276198	1.153730465396	6.210340963165
C	-1.568910763803	2.223608716193	6.570854380089
H	-3.635339625038	2.149651540734	3.825479219219
H	-0.183041256300	-0.321228774553	4.696669981056
H	-3.268091321244	3.433972916171	5.910453941815
H	0.191729700020	0.978998311338	6.828607604352
O	-1.315503051458	2.856270311078	7.727050166895
H	-1.871578751503	3.656134315879	7.825077587736
N	-4.304830636409	-3.056246268948	4.213042010937
C	-5.783659896372	-2.849059582399	4.158881261993
N	-6.268891034014	-2.680120694584	5.529898998126
C	-5.426134020752	-1.966895342488	6.434805695024
C	-5.285276182316	-0.499494009267	6.020241555417
O	-4.067485662519	0.012446362720	6.491109806468
O	-6.032701205404	0.170590711363	5.364224470104
H	-3.901850836646	0.933858526561	6.122508912741
C	-6.472673882712	-4.055514568983	3.493650770332
C	-4.748907329761	-7.186188412768	4.888193687912
C	-5.651017231916	-7.583731319486	5.890261101012
C	-5.033210722745	-6.067919009240	4.085602188772
H	-5.436250123547	-8.469408089779	6.506608425149
H	-4.344266959365	-5.793187096356	3.270038185172
C	-6.847398331053	-6.870579825557	6.073868804753
C	-6.223952961094	-5.328578121370	4.273302359382
H	-7.576307118444	-7.200823526821	6.829275195814
C	-7.131926227933	-5.751414608638	5.271306697301

H	-8.094686973009	-5.226557891382	5.390648631317
H	-3.830866837125	-7.767143747006	4.712290888037
C	-5.801514057612	-2.115794000306	7.943501211217
C	-3.760688505230	-3.292492286903	8.888978622137
C	-4.543118628608	-2.109935026431	8.789566770341
C	-2.532906367218	-3.295753900731	9.583528799872
H	-1.958855229960	-4.230233800546	9.675696587414
C	-4.058447661519	-0.931796038000	9.406520630462
C	-2.055895897518	-2.109621272574	10.179814280159
H	-4.655882376844	-0.008836928753	9.358909040913
H	-1.106299102046	-2.112050407856	10.735720019345
C	-2.822321003159	-0.929167229918	10.090073805308
H	-2.469764592074	-0.005932918447	10.574437052162
H	-4.131247462855	-4.228183944726	8.438975097939
H	-5.956253993225	-1.941239089605	3.553181428209
H	-6.321227197974	-3.088722083820	8.056599850488
H	-6.515515617357	-1.328979336826	8.255253213606
H	-6.083295709998	-4.121639447682	2.459344577954
H	-7.555235227889	-3.829147116710	3.429341049267
H	-4.027917571620	-3.887507672210	4.760028579575
H	-4.368346987016	-2.366171940668	6.397323266502
H	-6.565673660171	-3.586219416839	5.922934059113
N	-4.166715952047	-1.506714942350	1.866336640184
H	-4.521771191679	-0.758047199475	1.259933640028
H	-3.494661428430	-2.059061788301	1.318268207639
Pb	-2.092668108511	-1.434297300985	6.976427497864

YFF molecule + Cd^{2+}

C	-3.573537000000	-1.026254000000	3.254802000000
H	-4.286993000000	-0.355940000000	3.792134000000
C	-3.385060000000	-2.257926000000	4.164655000000
O	-2.318251000000	-2.413726000000	4.856017000000
C	-2.241093000000	-0.216112000000	3.080509000000
H	-1.427401000000	-0.902669000000	2.775011000000
H	-2.418176000000	0.479873000000	2.236165000000
C	-1.842841000000	0.577959000000	4.302071000000
C	-2.538642000000	1.751867000000	4.672025000000
C	-0.803266000000	0.150539000000	5.169111000000
C	-2.284062000000	2.433544000000	5.876116000000
C	-0.555081000000	0.797192000000	6.419022000000
C	-1.307802000000	1.954136000000	6.781228000000
H	-3.305806000000	2.160967000000	3.994499000000

H	-0.133195000000	-0.665196000000	4.849799000000
H	-2.826822000000	3.366405000000	6.100796000000
H	0.319839000000	0.528140000000	7.032817000000
O	-1.015584000000	2.520378000000	7.960792000000
H	-1.483237000000	3.373122000000	8.076277000000
N	-4.356274000000	-3.178711000000	4.209358000000
C	-5.841327000000	-2.926903000000	4.190542000000
N	-6.305575000000	-2.838341000000	5.568682000000
C	-5.444166000000	-2.145540000000	6.485363000000
C	-5.437875000000	-0.640580000000	6.205663000000
O	-4.190838000000	-0.083195000000	6.587683000000
O	-6.281786000000	0.047562000000	5.708044000000
H	-4.197322000000	0.881416000000	6.370047000000
C	-6.570733000000	-4.057819000000	3.445546000000
C	-4.978723000000	-7.366509000000	4.556729000000
C	-5.888339000000	-7.804109000000	5.534681000000
C	-5.216572000000	-6.171761000000	3.856096000000
H	-5.709492000000	-8.747476000000	6.071723000000
H	-4.522020000000	-5.859917000000	3.058876000000
C	-7.043948000000	-7.050877000000	5.799332000000
C	-6.367130000000	-5.395164000000	4.124282000000
H	-7.777509000000	-7.406718000000	6.538427000000
C	-7.282020000000	-5.855000000000	5.099319000000
H	-8.214431000000	-5.294381000000	5.280318000000
H	-4.090855000000	-7.971965000000	4.320366000000
C	-5.699990000000	-2.441876000000	7.992018000000
C	-3.233026000000	-2.653444000000	8.527292000000
C	-4.476746000000	-2.006923000000	8.771864000000
C	-2.014824000000	-2.116671000000	9.051008000000
H	-1.077931000000	-2.693558000000	8.956350000000
C	-4.484052000000	-0.888941000000	9.623491000000
C	-2.051801000000	-0.948161000000	9.860916000000
H	-5.440874000000	-0.394866000000	9.854077000000
H	-1.120295000000	-0.537740000000	10.277423000000
C	-3.289495000000	-0.368223000000	10.166320000000
H	-3.332915000000	0.507016000000	10.831613000000
H	-3.208203000000	-3.618272000000	7.991821000000
H	-5.984155000000	-1.972842000000	3.650160000000
H	-5.850110000000	-3.538586000000	8.083628000000
H	-6.621270000000	-1.945489000000	8.352069000000
H	-6.189970000000	-4.063950000000	2.406005000000
H	-7.644922000000	-3.789505000000	3.406001000000
H	-4.103087000000	-4.034995000000	4.728787000000

H	-4.384081000000	-2.457533000000	6.342888000000
H	-6.582670000000	-3.765515000000	5.924356000000
N	-4.237733000000	-1.441998000000	2.037001000000
H	-4.551045000000	-0.642022000000	1.475485000000
H	-3.636508000000	-2.029653000000	1.445587000000
Cd	-2.115386000000	-1.213210000000	6.734576000000

YFF molecule + Hg^{2+}

C	-3.556596711357	-1.090485035099	3.145569686626
H	-4.337980479704	-0.481009941811	3.653055699670
C	-3.324590759228	-2.350375169523	4.012209300142
O	-2.218027863034	-2.539683267406	4.593829186235
C	-2.247041245780	-0.219331843237	3.102781238395
H	-1.389260738837	-0.876650058772	2.863866684718
H	-2.381821092188	0.487918697985	2.260812639056
C	-1.972807750582	0.585283874534	4.343151966866
C	-2.670001189821	1.784605347738	4.596916184810
C	-0.946692291101	0.221989578375	5.294076558983
C	-2.359788934198	2.615328282793	5.686019538021
C	-0.597268023400	1.096424901444	6.384483116650
C	-1.317346071008	2.289479533140	6.595439689049
H	-3.449404611500	2.115581898879	3.892342126201
H	-0.220405976797	-0.555754359071	4.995744280892
H	-2.906695550831	3.565064462153	5.810666385984
H	0.262751181493	0.868175314255	7.032622309344
O	-0.958369564131	3.054615419102	7.636091752795
H	-1.423941610746	3.915481063260	7.631376351145
N	-4.335314904453	-3.235016620107	4.112681582491
C	-5.800172289388	-2.931425722297	4.104860943676
N	-6.251974579676	-2.738599030996	5.475947052515
C	-5.390819314799	-1.987669835041	6.348791554097
C	-5.450083418779	-0.484516051190	6.056380532830
O	-4.507892279037	0.188366424863	6.814363941169
O	-6.123912125238	0.072855023792	5.226048705823
H	-4.549652357381	1.136849809983	6.548975554674
C	-6.580058459514	-4.081930106344	3.442046827607
C	-5.050559212705	-7.376201427402	4.678012175726
C	-5.943456164863	-7.736963857494	5.701662900471
C	-5.275485055850	-6.212005521596	3.924426172163
H	-5.777121759759	-8.657974915939	6.279944632197
H	-4.598225216747	-5.962077368930	3.091535127073
C	-7.070116624215	-6.937020723265	5.959120748211

C	-6.395380960306	-5.387457458736	4.185065598496
H	-7.791566069816	-7.234159845495	6.735143193884
C	-7.294834182415	-5.771267290869	5.206371958026
H	-8.205114377809	-5.174577695878	5.383668450390
H	-4.187705031442	-8.019233697050	4.447944851825
C	-5.575976893184	-2.322637203833	7.852103674980
C	-3.086394381335	-2.643400622448	8.388232606918
C	-4.355337878356	-2.016802612669	8.689731119133
C	-1.949297011535	-2.436140100630	9.256150777328
H	-1.025723912523	-3.009614941747	9.075625008118
C	-4.412219994848	-1.160732229721	9.795690044745
C	-2.046684856990	-1.559173882279	10.342094882603
H	-5.364904586529	-0.673274179507	10.052043083213
H	-1.182384531146	-1.393858237530	11.001387780210
C	-3.279333582964	-0.933519172341	10.608175264454
H	-3.370602145407	-0.265530656121	11.478678403194
H	-3.077331893374	-3.534852346089	7.733229633889
H	-5.931603481463	-2.009527674453	3.510272592154
H	-5.767429137036	-3.416783926864	7.911169362211
H	-6.470213148715	-1.817095781610	8.264413641214
H	-6.226787676705	-4.159594460221	2.395491292962
H	-7.647373193375	-3.786713662740	3.414257904943
H	-4.094146279980	-4.100847640105	4.621659376016
H	-4.319774533623	-2.239684830617	6.139758470632
H	-6.530014852987	-3.638768311314	5.891851775074
N	-4.102153096525	-1.493626172016	1.875520725106
H	-4.491703515098	-0.722345924090	1.323250687195
H	-3.457506565171	-2.045447338420	1.297654760612
Hg	-2.115400184192	-1.243306881380	6.723168934174

16.0 Refereces:

[1] R. Singh, N. K. Mishra, V Kumar, V. Vinayak, K. B. Joshi, *ChemBioChem.*, **2018**, 19, 1630–1637.

[2] N. Singh, R. Singh, M. Shukla, G. Kaul, S. Chopra, K. B. Joshi, S. Verma, *ACS Infect. Dis.*, **2020**, 6, 2441-2450.

[3] N. Singh, S. Sharma, R. Singh, S. Rajput, N. Chatopadhya, D. Tiwari, K. B. Joshi, S.Verma, *Chem. Sci.*, **2021**, 12, 16085-16091.

[4] N. K. Mishra, K. B. Joshi**,** S. Verma, *J. Colloid. Inter. Sci.*, **2015**, 455, 145

[5] N. K. Mishra, V. Kumar, K. B. Joshi, *Nanoscale.*, **2015**, 7, 20238–20248.

[6] R. Singh, N. K. Mishra, P. Gupta, K. B. Joshi, *Chem. Asian J.*, **2020**, 15, 531–539.

[7] R. Singh, N. K. Mishra, N. Singh, P. Rawal, P. Gupta, K. B. Joshi, *New J. Chem.,* **2020**, 44, 9255—9263.

[8] K. Kesharwani, R. Singh, M. J. Khan, V. Vinayak, K. B. Joshi, *ChemistrySelect.*, **2021**, 6, 6827 - 6833.

[9] F. Neese, *Comput. Mol. Sci.,* **2012**, 2 (1), 73-78.. Neese,. *Comput. Mol. Sci.*, **2022**, 12, e1606.

[10] (a) A. D. Becke, *Phys. Rev. A.*, **1988**, 38 (6), 3098-3100 (b) J. P. Perdew, *Phys. Rev. B.*, **1986**, 33 (12), 8822.

[11] F. Weigend, R. Ahlrichs, *Phys. Chem. Chem. Phys.*, **2005**, 7 (18), 3297-3305.

[12] S.Grimme, S. Ehrlich, L. Goerigk, *J. Comput. Chem.*, **2011**, 32, (7) 1456-1465.

[13] J. Tomasi, B. Mennucci, R. Cammi, *Chem. Rev.,* **2005**, 105 (8), 2999-3094.